



Available online at [www.sciencedirect.com](http://www.sciencedirect.com)

ScienceDirect

[www.elsevier.com/locate/jes](http://www.elsevier.com/locate/jes)



# Challenges to quantitative applications of Landsat observations for the urban thermal environment

Feng Chen<sup>1,2,3,\*</sup>, Song Yang<sup>1,2</sup>, Kai Yin<sup>4</sup>, Paul Chan<sup>5</sup>

1. School of Atmospheric Sciences, Sun Yat-sen University, Zhuhai 519082, China. Email: [chenfeng105@gmail.com](mailto:chenfeng105@gmail.com)
2. Institute of Earth Climate and Environment System, Sun Yat-sen University, Guangzhou 510275, China
3. Fujian Key Laboratory of Sensing and Computing for Smart City, Xiamen University, Xiamen 361005, China
4. Institute of Remote Sensing and Digital Earth, Chinese Academy of Sciences, Beijing 10094, China
5. Climate Decision LLC, Bethesda, MD, USA

## ARTICLE INFO

### Article history:

Received 25 November 2016  
 Revised 14 February 2017  
 Accepted 16 February 2017  
 Available online 24 February 2017

### Keywords:

Remote sensing  
 Radiometric calibration  
 SLC-off  
 Surface temperature  
 Data consistency

## ABSTRACT

Since the launch of its first satellite in 1972, the Landsat program has operated continuously for more than forty years. A large data archive collected by the Landsat program significantly benefits both the academic community and society. Thermal imagery from Landsat sensors, provided with relatively high spatial resolution, is suitable for monitoring urban thermal environment. Growing use of Landsat data in monitoring urban thermal environment is demonstrated by increasing publications on this subject, especially over the last decade. Urban thermal environment is usually delineated by land surface temperature (LST). However, the quantitative and accurate estimation of LST from Landsat data is still a challenge, especially for urban areas. This paper will discuss the main challenges for urban LST retrieval, including urban surface emissivity, atmospheric correction, radiometric calibration, and validation. In addition, we will discuss general challenges confronting the continuity of quantitative applications of Landsat observations. These challenges arise mainly from the scan line corrector failure of the Landsat 7 ETM+ and channel differences among sensors. Based on these investigations, the concerns are to: (1) show general users the limitation and possible uncertainty of the retrieved urban LST from the single thermal channel of Landsat sensors; (2) emphasize efforts which should be done for the quantitative applications of Landsat data; and (3) understand the potential challenges for the continuity of Landsat observation (i.e., thermal infrared) for global change monitoring, while several climate data record programs being in progress.

© 2017 The Research Center for Eco-Environmental Sciences, Chinese Academy of Sciences.

Published by Elsevier B.V.

## Contents

Introduction . . . . .	81
1. The single-channel method for LST retrieval . . . . .	82
2. Challenges for the quantitative application over urban area . . . . .	83
2.1. Urban surface emissivity . . . . .	83

\* Corresponding author.

2.2. Atmospheric correction . . . . . 83  
 2.3. Radiometric calibration . . . . . 84  
 2.4. Validation. . . . . 84  
 2.5. Other issues . . . . . 84  
 3. New strategies for LST retrieval over urban areas . . . . . 85  
 4. Conclusions. . . . . 86  
 Acknowledgement. . . . . 86  
 References . . . . . 86

**Introduction**

The Landsat program, jointly operated by the National Aeronautics and Space Administration (NASA) and the U. S. Geological Survey (USGS), has been collecting space-based imagery with moderate spatial resolution of the Earth’s surface since the launch of its first satellite in 1972. This series of land-observing satellites has created a historical archive that is unmatched in quality, spatial coverage, and length. Landsat 8, launched on 11 February 2013, is the newest satellite in the Landsat program. Furthermore, NASA and USGS have started work on Landsat 9, which is planned to be launched in 2023. Landsat 9 will extend the Landsat program to half a century (NASA, 2015a). Furthermore, the Landsat program will potentially be sustained operationally further by Landsat 10 (Loveland and Dwyer, 2012).

The spatial resolution of Landsat observation is important. On the one hand it is coarse enough for continuous global coverage, and on the other hand it is detailed enough to characterize human-scale processes. With the use of Landsat observations, it is possible to investigate human interactions with the environment in a global scale (NASA, 2015b). At present, the data collected for over more than forty years by the Landsat program provide a unique database for global change research. The continuity characterized with consecutive, temporally overlapping observations and cross-sensor calibration, makes Landsat observation an important asset for climate studies (Trenberth et al., 2013). Furthermore, thanks to the free data policy (Woodcock et al., 2008; Loveland and Dwyer, 2012) the Landsat data have been adopted in a wide range of studies and applications. Accordingly, the Landsat program has significantly benefited both the academic community and societal applications such as the management of water, land, forest, wildlife, and natural hazards. The annual economic benefits in 2011 obtained from the Landsat imageries were estimated to be \$2.19 billion, although this estimate may be conservative (Loomis et al., 2015).

So far, the thermal images acquired by Landsat sensors, including the Thematic Mapper (TM) on-board Landsat 4/5, the Enhanced Thematic Mapper Plus (ETM+) on-board Landsat 7, and the Thermal Infrared Sensor (TIRS) on-board Landsat 8, have high spatial resolution (Table 1) for monitoring urban thermal environment (Sobrino et al., 2012; Xiao et al., 2007), especially when compared with the coarser-resolution thermal images collected by AVHRR (or Advanced Very High Resolution Radiometer) and MODIS (or MODerate Resolution Imaging Spectroradiometer). Landsat 4 was operated over 10 years from 1982 to 1993. Landsat 5 successfully collected

data from its launch in 1984 until the communication system failures in November 2011, and finally went out of commission in June 2013 (USGS, 2013b). Landsat 7, launched in April 1999, has acquired observations for more than 17 years so far. Actually, a thermal channel was firstly embedded in Landsat 3 MSS; however, its poor performance and few data-acquisition make application of its data impossible (Arvidson et al., 2013). Compared with its predecessors, Landsat 8 has two separate push-brooms scanners, including the Operational Land Imager (OLI) and the TIRS. Specifically, the OLI has two additional channels provided with narrower bandwidths (i.e., Band 1 and Band 9), while the TIRS has two thermal channels in the range of 10.0–13.0 μm (Table 1). Relative spectral responses (RSRs) for the channels are shown in Figs. 1 and 2. The two new bands of Landsat 8 OLI are not shown in Fig. 1. Effective wavelengths

**Table 1 – General information about the Landsat sensors.**

	Landsat 4/5 TM	Landsat 7 ETM+	Landsat 8 OLI/TIRS
Visible (μm)	0.45–0.52 (30 m)	0.45–0.52 (30 m)	0.45–0.51 (30 m)
	0.52–0.60 (30 m)	0.52–0.60 (30 m)	0.53–0.59 (30 m)
	0.63–0.69 (30 m)	0.63–0.69 (30 m)	0.64–0.67 (30 m)
Near infrared	0.76–0.90 (30 m)	0.77–0.90 (30 m)	0.85–0.88 (30 m)
Short-wave infrared	1.55–1.75 (30 m)	1.55–1.75 (30 m)	1.57–1.65 (30 m)
	2.08–2.35 (30 m)	2.09–2.35 (30 m)	2.11–2.29 (30 m)
Panchromatic		0.52–0.90 (15 m)	0.50–0.68 (15 m)
Thermal infrared	10.40–12.50 (120 m <sup>a</sup> )	10.40–12.50 (60 m <sup>b</sup> )	10.60–11.19 (100 m <sup>c</sup> )
			11.50–12.51 (100 m)
[Band 1]			0.43–0.45 (30 m)
[Band 9]			1.36–1.38 (30 m)

Compared with its predecessors, Landsat 8 has two new bands, including a band (Band 1, 0.43–0.45 μm) useful for coastal and aerosol studies and a band (Band 9, 1.36–1.39 μm) useful for cirrus cloud detection. Values in parentheses in Table 1 are spatial resolutions of the specific thermal images. The resolution for ETM+ and OLI panchromatic bands of is 15 m, and the spatial resolution for other spectral bands located within visible, near infrared, and short-wave infrared regions is 30 m. Information in Table 1 is obtained from [http://landsat.usgs.gov/band\\_designations\\_landsat\\_satellites.php](http://landsat.usgs.gov/band_designations_landsat_satellites.php).

<sup>a</sup> TM thermal band was originally acquired at 120 m resolution. But, products processed before February 25, 2010 are resampled to 60 m pixels, while products processed after February 25, 2010 are resampled to 30 m pixels.

<sup>b</sup> ETM+ thermal band is acquired at 60 m resolution. Products processed after February 25, 2010 are resampled to 30 m pixels.

<sup>c</sup> TIRS thermal bands are acquired at 100 m resolution, but are resampled to 30 m in delivered data product.

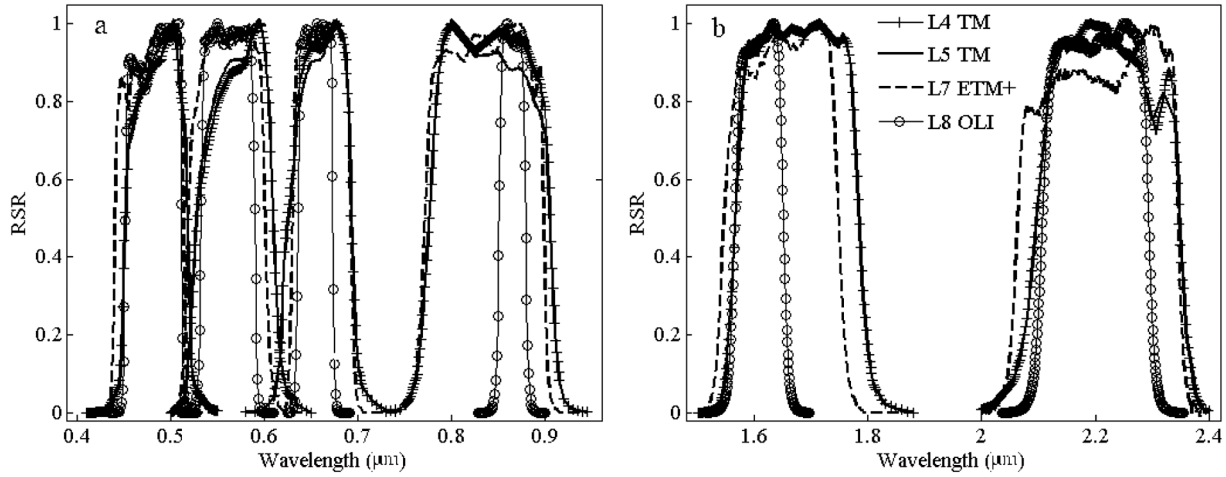


**Fig. 1 – Relative spectral responses (RSRs) for Landsat channels within (a) the visible and near infrared regions and (b) the short-wave infrared regions.**

for thermal channels given in Fig. 2 are 11.154 μm (Landsat 4 TM), 11.457 μm (Landsat 5 TM), 11.269 μm (Landsat 7 ETM+), 10.904 μm (Landsat 8 TIRS1), and 12.003 μm (Landsat 8 TIRS2). The effective wavelengths are obtained through a “Trapezoid” strategy (Hu et al., 2011). All RSRs used are described in <https://landsat.usgs.gov/instructions.php>.

According to the Web of Science™, publications of Landsat applications on urban heat island effect have increased significantly over the last two decades. For example, when the “Landsat”, “Thermal”, and “Urban heat island” are used jointly as keywords, search results (on 10 February 2017) show 155 publications during 2011–2016 while only 6 publications during 1995–2000 ([http://apps.webofknowledge.com/WOS\\_GeneralSearch\\_input.do?product=WOS&SID=3Fe6XEUKTRqj5YuOBKd&search\\_mode=GeneralSearch](http://apps.webofknowledge.com/WOS_GeneralSearch_input.do?product=WOS&SID=3Fe6XEUKTRqj5YuOBKd&search_mode=GeneralSearch)). The significant increase in publications suggests the growing availability and interests in Landsat data for investigating urban thermal environment. The increase applications of Landsat data also reminds us the issues associated with data quality and accuracy. Major concerns discussed here are on the challenges confronting the continuity of quantitative applications of Landsat observations in urban thermal environment, which is usually represented by land surface temperature (LST). However, it is not intended to review all publications, rather it is

to show readers and data users several related aspects, which include urban surface emissivity, atmospheric correction, radiometric calibration, and other issues (i.e., data gaps, sensor differences, validation, and data/products consistency). At last, two new strategies are proposed to overcome the challenges in LST retrieval from single thermal channel imagery, which are specifically in the requirements of atmospheric parameters and emissivity.

## 1. The single-channel method for LST retrieval

The single-channel method (Jiménez-Muñoz and Sobrino, 2003) is generally the only way to obtain LST from Landsat thermal imagery (i.e., Landsat 4/5 TM and Landsat 7 ETM+), except for Landsat 8 TIRS, which has two thermal infrared channels (Table 1 and Fig. 2). However, calibration uncertainties of Landsat 8 TIRS are more obvious, especially for TIRS2, compared with the thermal channels of its predecessors (Barsi et al., 2014). Accordingly, the single-channel method can be used for Landsat 8 at present, when TIRS1 is usable (Barsi et al., 2014). Based on the single-channel algorithm (Jiménez-Muñoz and Sobrino, 2003), LST can be obtained by Eqs. (1)–(3).

$$T_s = \gamma \left[ \frac{1}{\varepsilon_e} (\psi_1 L_{\text{obs}} + \psi_2) + \psi_3 \right] + \delta \quad (1)$$

$$\gamma = \left[ \frac{C_2 L_{\text{obs}}}{T_{\text{obs}}^2} \left( \frac{\lambda_e^4}{C_1} L_{\text{obs}} + \frac{1}{\lambda_e} \right) \right]^{-1} \quad (2)$$

$$\delta = T_{\text{obs}} - \gamma L_{\text{obs}} \quad (3)$$

where  $L_{\text{obs}}$  ( $\text{W}\cdot\text{m}^{-2}\cdot\text{sr}^{-1}\cdot\mu\text{m}^{-1}$ ) is the at-sensor radiance, and  $T_{\text{obs}}$  (K) is the at-sensor brightness temperature.  $\lambda_e$  ( $\mu\text{m}$ ) is the effective wavelength, and  $\varepsilon_e$  is the surface emissivity.  $\gamma$  and  $\delta$  are two parameters related to the Planck’s law, whereas  $\psi_1$ ,  $\psi_2$  ( $\text{W}\cdot\text{m}^{-2}\cdot\text{sr}^{-1}\cdot\mu\text{m}^{-1}$ ), and  $\psi_3$  s ( $\text{W}\cdot\text{m}^{-2}\cdot\text{sr}^{-1}\cdot\mu\text{m}^{-1}$ ) are atmospheric functions which can be estimated using

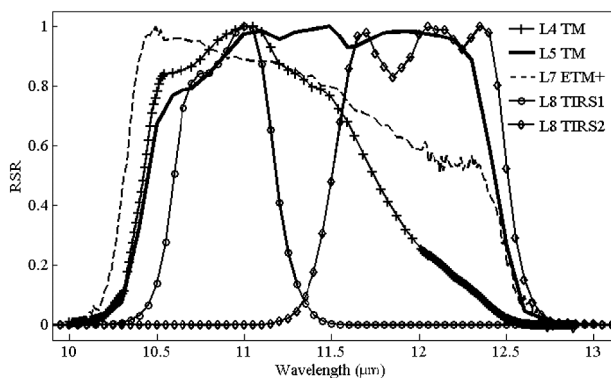


**Fig. 2 – RSRs for the Landsat thermal channels.**

atmospheric water vapor content (Jiménez-Muñoz and Sobrino, 2003). Two constants are  $c_1 = 1.19104 \times 10^8 \text{ W} \cdot \mu\text{m}^4 \cdot \text{m}^{-2} \cdot \text{sr}^{-1}$  and  $c_2 = 14387.7 \text{ } \mu\text{m}/\text{K}$ .

For the widely used single-channel algorithm (Jiménez-Muñoz and Sobrino, 2003), the required inputs include surface emissivity, atmospheric water vapor content, and well calibrated radiance. However, in most cases, especially for general users, it is impossible to obtain these inputs accurately (Chen et al., 2014a, 2014b, 2015).

## 2. Challenges for the quantitative application over urban area

### 2.1. Urban surface emissivity

Most urban surfaces consist of different manmade materials with distinct reflectance and thermal emission. This results in significant challenges in urban LST retrieval caused by the uncertainty of urban surface emissivity estimation, especially when single-channel method is used (Chen et al., 2016a; Yang et al., 2015). The influences of emissivity uncertainty on LST retrieval are regulated by climate and geography backgrounds (Chen et al., 2016a). Generally, the uncertainty in surface emissivity should be less than 0.01 to achieve a high accuracy in the final LST estimation (about 0.5 K), whereas a 0.02 uncertainty in surface emissivity may cause a LST error larger than 1.0 K. A more obvious LST error may be resulted in under a dry and warm condition (Chen et al., 2016a; Valor and Caselles, 1996; Trigo et al., 2008).

Emissivity variation of manmade materials is shown by the box plot in Fig. 3, which is based on the spectra samples from the ASTER Spectral Library Version 2.0 (Baldrige et al., 2009). Totally, 36 spectra of manmade materials are selected in this paper, mainly considering the differences of wavelength coverage between the channels' RSRs and the spectra. Generally, obvious emissivity variation is recorded, and the variation amplitude (range between the two whiskers in the box plot, Fig. 3) is approximately 0.1 for each individual thermal channel. The emissivity variation suggests that it is difficult to determine a suitable value to represent the emissivity of manmade materials over urban area. For about a

half of these selected samples, the emissivity uncertainty is more than 0.02 if the median value is used as the representative emissivity. Accordingly, a larger LST error (>1.0 K) occurs in about 50% of the samples. However, the findings based on the ASTER Spectral Library Version 2.0 here just provide an incomplete insight into the challenges associated with urban surface emissivity. Furthermore, widely used approaches, in particular, the classification-based method and the vegetation index-based method, are likely unable to meet the demands for accurate estimation of urban surface emissivity (Chen et al., 2016a). Currently, the spectra (i.e., manmade materials) available for urban remote sensing are limited, with respect to spectral resolution, spectral domain as well as the number of samples. Accordingly, more spectra of manmade materials covering more diverse urban settings are needed (Chen et al., 2016a).

Over urban areas characterized by heterogeneous landscape, the surface thermal anisotropy is generally significant (Voogt and Oke, 1998, 2003; Lagouarde et al., 2004, 2010; Sun et al., 2015). The angular variation of surface emissivity and the relative fractions of different components (e.g., the presence of vegetation) within the instantaneous field of view will result in directional LST variation (Lagouarde et al., 2004). Meanwhile, the variability of microscale temperature makes substantial contributions to the thermal anisotropy (Voogt, 2008). Additionally, effects caused by urban geometry should be taken into account in urban LST estimation (Yang et al., 2015). It becomes a complicated issue that obtaining urban LST from remote sensing data (Voogt and Oke, 2003), in particular, for the retrieval from only one thermal band (e.g., Landsat 4/5 TM and Landsat 7 ETM+).

### 2.2. Atmospheric correction

Atmospheric correction is important for LST retrieval from Landsat observation. For the current single-channel method, atmospheric water vapor content is a necessary input (Jiménez-Muñoz and Sobrino, 2003). Meanwhile, atmospheric heterogeneity is always demonstrated at regional scale (Chen et al., 2010a). However, atmospheric correction and the heterogeneity of atmosphere have always been ignored, or the atmospheric parameters acquired at one station/site were

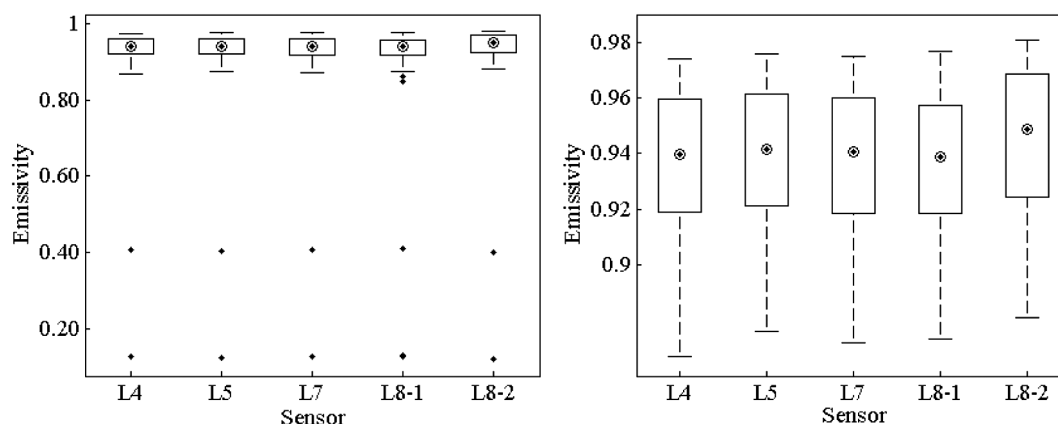


Fig. 3 – The effective emissivity of manmade materials spectra selected from ASTER Spectral Library Version 2.0. The right figure presents the enlarged plots correspondingly (with the vertical axis ranging from 0.86–0.99).

used as the representative value over the entire image (Chen et al., 2010a). The MODIS standard atmospheric products, including MOD 05 and MOD 07, are considered good resources for atmospheric correction (Chen et al., 2010a, 2011a; Li et al., 2007; Jiménez-Muñoz et al., 2010). However, obvious uncertainty in the MODIS standard products (Meng et al., 2007) may make the atmospheric correction uncertain. Using MODIS atmospheric products for atmospheric correction improves the final LST accuracy for some cases (Chen et al., 2010a, 2011a, Jiménez-Muñoz et al., 2010) while it does not show any benefits for other cases (Chen et al., 2015). This uncertainty may hamper the application of MODIS atmospheric products in atmospheric correction. Findings indicate the necessity to validate and improve MODIS atmospheric products before application (Chen et al., 2015).

### 2.3. Radiometric calibration

Radiometric calibration is the procedure for obtaining the at-sensor radiance from digital records (i.e., digital number records) to generate brightness temperature and the final LST retrieval (see Eqs. (1)–(3)). Uncertainty in radiometric calibration usually becomes increasingly obvious as the sensor decays during in-orbit operation. Radiometric problems were found in Landsat sensors (Barsi et al., 2006, 2007, 2014; Markham and Helder, 2012). According to radiative transfer model, a sensitivity model to assess impacts of the uncertainty in radiometric calibration on LST retrieval is obtained (Chen et al., 2016b):

$$\Delta T_s = \frac{\partial T_s}{\partial B(T_s)} \frac{1}{\tau \epsilon_e} \Delta L_{\text{obs}} \quad (4)$$

where  $\Delta L_{\text{obs}}$  ( $\text{W}\cdot\text{m}^{-2}\cdot\text{sr}^{-1}\cdot\mu\text{m}^{-1}$ ) is the radiometric calibration error, and  $\Delta T_s$  (K) is the LST uncertainty resulted from radiometric calibration error.  $\tau$  is the atmospheric transmissivity.  $\frac{\partial T_s}{\partial B(T_s)}$  showing the relationship between LST and radiance (as derivation) can be obtained according to the Planck's law, through a numerical simulation (Chen et al., 2016b).

Investigations show that a 0.1 unit ( $\text{W}\cdot\text{m}^{-2}\cdot\text{sr}^{-1}\cdot\mu\text{m}^{-1}$ ) error of the radiometric calibration may result in a LST error of approximately 1.0 K for a moderate case (Chen et al., 2016b). As shown in previous findings, an average error in radiometric calibration of TM during 1999–2006 was about  $0.12 \text{ W}\cdot\text{m}^{-2}\cdot\text{sr}^{-1}\cdot\mu\text{m}^{-1}$  (Barsi et al., 2006). Uncertainty in the radiometric calibration of Landsat 8 TIRS is still obvious, specifically for TIRS1 and TIRS2, in which the calibration errors are within  $\pm 0.12 \text{ W}\cdot\text{m}^{-2}\cdot\text{sr}^{-1}\cdot\mu\text{m}^{-1}$  and  $\pm 0.20 \text{ W}\cdot\text{m}^{-2}\cdot\text{sr}^{-1}\cdot\mu\text{m}^{-1}$ , respectively (Barsi et al., 2014). The calibration of Landsat 8 TIRS bands is not truly correct until the stray light contribution is removed (Barsi et al., 2014).

### 2.4. Validation

Validation is the comparison of retrieved results with reference data to assess retrieval quality, which is a critical and significant procedure to ensure the retrieved results are suitable for the desired applications (Rizwan et al., 2008; Li et al., 2013). The accuracy and precision of the retrieved results are determined through the validation procedure,

provided that the errors or uncertainties in the reference data are fully understood and accounted for (Hollmann et al., 2013). Generally, the validation procedure is conducted by directly comparing the retrieved results with *in situ* measurements. However, the direct validation is often limited with respect to (1) spatio-temporal coverage of *in situ* observations and (2) the scale contrast/difference between satellite records and *in situ* measurements (Zeng et al., 2015). Moreover, the locations of *in situ* measurements are often biased (e.g., located within a certain land cover type) (Camacho et al., 2013; Oltra-Carrió et al., 2012). Thus, in practice, indirect validation, in which other products are used as the reference, is often conducted (Chen et al., 2015; Zeng et al., 2015). When the indirect validation is used, however, we need to make sure how the reference data is generated. If the data served as reference suffer from limitations and uncertainties, comparison and validation should be used with caution. Accordingly, a validation with professional guidelines is essential (Zeng et al., 2015).

In particular, for urban areas which are covered by mixture of diverse materials with complicated composition and geometry, it is difficult to obtain sufficient *in situ* measurements for validation purpose. In Oltra-Carrió et al. (2012), validation data are obtained at four sites, of which two are building roofs. Long term records with large coverage for validation purpose are even less. To solve the spatial coverage issue of *in situ* data, thermal imagery with high spatial resolution collected by satellite or airborne sensors can be used (Voogt, 2008). However, the limitation of flight campaign is usually associated with the limited temporal coverage (Zeng et al., 2015) and the geometric rectification issues inherent in airborne sensed data (Gluch et al., 2006).

### 2.5. Other issues

Normalized Difference Vegetation Index (NDVI, Eq. (5)) is a widely used indicator for mapping and monitoring vegetated areas using multispectral remotely sensed data. Meanwhile, Normalized Difference Built-Up Index (NDBI, Eq. (6)) is used to map built-up areas through a quick and objective process (Zha et al., 2003). Both NDVI and NDBI were used as indicators to characterize urban landscape and to model urban thermal environment, such as in Xiao et al. (2007) and Xiong et al. (2012).

$$\text{NDVI} = \frac{\rho_{\text{NIR}} - \rho_{\text{Red}}}{\rho_{\text{NIR}} + \rho_{\text{Red}}} \quad (5)$$

$$\text{NDBI} = \frac{\rho_{\text{SWIR}} - \rho_{\text{NIR}}}{\rho_{\text{SWIR}} + \rho_{\text{NIR}}} \quad (6)$$

where  $\rho_{\text{Red}}$ ,  $\rho_{\text{NIR}}$ , and  $\rho_{\text{SWIR}}$  refer to surface reflectance values of Band 3, Band 4, and Band 5 of Landsat 4/5 TM and Landsat 7 ETM+, while they refer to Band 4, Band 5, and Band 6 of Landsat 8 OLI (Table 1), respectively.

As shown by the spectra of manmade materials selected from the ASTER Spectral Library Version 2.0, minor differences in both NDVI and NDBI are shown between Landsat 4/5 TM and Landsat 7 ETM+, with absolute discrepancy being less than 0.002. However, more significant differences in both NDVI and NDBI exist between Landsat 8 OLI and its predecessors (i.e., Landsat 4/5 TM and Landsat 7 ETM+) (Fig. 4). The obvious variation in sensor settings between the

Landsat 8 OLI and its predecessors, as shown in Fig. 1, may be the main cause for the between-sensors discrepancies. The between-sensors discrepancies may become more significant in applications when atmospheric impacts and land cover conditions are considered (Li et al., 2014). Differences in measuring vegetation indices among Landsat sensors have been investigated (Li et al., 2014; Xu and Guo, 2014), whereas related investigations on NDBI have not been discussed widely yet.

At the same time, differences are there in spatial resolution among the thermal channels, although the data (i.e., Level 1 T) are provided after being re-sampled to 30 m resolution currently (Table 1). According to the header file and Chander et al. (2009), a cubic convolution method is used in the re-sampling procedure. It is necessary to investigate whether artifacts are introduced during the re-sampling procedure, considering the complexity of the urban surface heterogeneity and the scaling effect in urban thermal environment (Chen et al., 2008; Liu and Weng, 2009; Pu et al., 2006). Landsat 8 TIRS data, acquired with improved Signal-to-Noise Ratio, are delivered with 30 m resolution and with a 16-bit radiometric quantization range (i.e., Level 1 T, see USGS, 2013a). Meanwhile, the Landsat 4/5 TM and Landsat 7 ETM+ thermal channel images are delivered with 8-bit range (Chander et al., 2009). The quantization level is “the number of numerical values used to represent a continuous quantity” (USGS, 2015b). The disparities in radiometric quantization and different gain modes may affect the comparability among different sensors (or channels) in view of absolute values (Liu et al., 2011). Uncertainty caused by the differences of sensor settings may hamper direct comparison among Landsat sensors, which makes continuity of quantitative applications difficult. Therefore, related uncertainty should be eliminated, especially when precise surface change detection or temporal is needed.

The Scan Line Corrector (SLC) of Landsat 7 ETM+ has failed since 31 May 2003. This SLC failure (SLC-off) has limited the quantitative applications of Landsat 7 ETM+ data to some extent. What is worse, Landsat 5 TM had been suspended since November 2011, resulting from the failure of its electronic component that is vital to data transmission. Landsat 5 was finally terminated on 5 June 2013 (USGS, 2013b). The data gap resulted from these problems may affect the continuity

of Landsat program, even the Earth observation. Currently, Landsat higher level science data products provided publicly include “surface reflectance higher level data products” and “surface reflectance-derived spectral indices” (USGS, 2015a). However, the Landsat 7 ETM+ SLC-off data, used as inputs for higher level products, are still not gap-filled. Several approaches have been proposed to resolve the SLC-off issue (Scaramuzza and Micijevic, 2004; USGS and NASA, 2004; Chen et al., 2010b, 2011c). Relatively much attention has been paid to the multispectral bands, whereas a few investigations have been conducted for the thermal channel (Chen et al., 2011b, 2012). However, the uncertainty resulted from recovering procedure should not be ignored (Chen et al., 2011b). More efforts are needed to find proper and robust solutions for the SLC failure, mainly due to both the valuable legacy of the Landsat series and the data open policy (Woodcock et al., 2008; Loveland and Dwyer, 2012).

Furthermore, spatial patterns of urban LST show differences between daytime and nighttime observations (i.e., diurnal variations) (Buyantuyev and Wu, 2010; Rizwan et al., 2008). Therefore, representative LST observations throughout the diurnal cycle should be acquired (Sobrino et al., 2012). Unfortunately, due to inefficiency of its temporal coverage, LST derived from Landsat observation may be less useful for assessing shorter-term urban thermal environment, such as the condition during heat events (White-Newsome et al., 2013).

### 3. New strategies for LST retrieval over urban areas

As mentioned above, for the current single-channel method, valid surface emissivity and atmospheric water vapor content are necessary prerequisites (see Section 2.1 and Section 2.2). However, usually, surface emissivity and atmospheric parameters are not readily accessible to general users (Chen et al., 2014b, 2015). When variables estimated from remote sensing imagery are used as inputs for LST retrieval, their uncertainties are often ignored. These difficulties can possibly limit the application of current single-channel algorithms (Chen et al., 2014b). Therefore a new retrieval methodology is needed. Two innovative approaches have been developed, including the single-channel

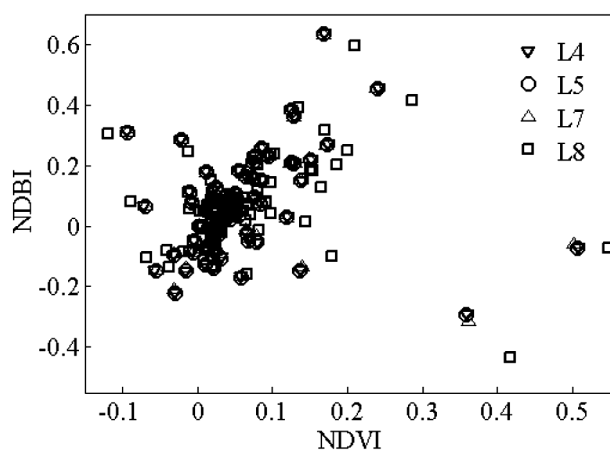


Fig. 4 – Scatter plot of Normalized Difference Vegetation Index (NDVI) and Normalized Difference Built-Up Index (NDBI) for selected manmade spectra.

method based on temporal and spatial information (MTSC) (Chen et al., 2014b) and the image based single-channel method (IBSC) (Chen et al., 2015). These newly developed methods are for estimating LST accurately from at-sensor radiance observed by one thermal channel, even without any accurate information about the atmospheric parameters and land surface emissivity (Chen et al., 2014a, 2014b, 2015). Preliminary results show good performances of the new methods, although currently only the HJ-1B cases have been shown. Further investigations are being undertaken to refine these innovative methodologies for Landsat sensors. How to ensure retrieval accuracy and consistency is critical to quantitative applications of these methods. However, a retrieval method possibly shows varied performances in different cases (e.g., temporal differences, and different climatological and geographical conditions).

#### 4. Conclusions

Thermal imagery from Landsat sensors (i.e., Landsat 4/5 TM, Landsat 7 ETM+, and Landsat 8 TIRS) has been widely used for urban thermal environment (Weng, 2009). However, quantitative application of the thermal imagery is always limited. This is due mainly to the inaccessibility to adequate information about the atmosphere and the urban heterogeneity with respect to surface emissivity and reflectance, as well as problems in radiometric calibration and validation. Additionally, to take advantage of the outstanding legacy of the Landsat program, challenges related to sensor decay, the differences of settings among sensors, as well as the Landsat 7 ETM+ SLC-off problem are noteworthy. The consistency and accuracy of retrieved products, as well as the continuity of data collection, are critical for desired investigations. However, in most case studies, quantitative retrieval results are not guaranteed and even not assessed fully, due mainly to the inaccessibility to adequately proper reference data for validation.

Several climate data records (CDRs) programs are in progress, which are intended to produce trustworthy information on global and regional changes (Hollmann et al., 2013; USGS, 2015a; NOAA, 2015; NASA, 2015c; Zeng et al., 2015). USGS is capitalizing on the valuable Landsat time series to generate higher level data products (USGS, 2015a). Currently, two higher level Landsat products are available publicly, including “surface reflectance higher level data products” and the “surface reflectance-derived spectral indices”. Several other higher level products, including LST, are being planned for the future ([https://landsat.usgs.gov/CDR\\_ECV.php](https://landsat.usgs.gov/CDR_ECV.php)). Merits of these products are significant, but the importance of product quality and consistency is necessarily to be emphasized, as shown by the definition of CDR (NRC, 2004), considering their potential applications for quantitative investigations such as for monitoring urban thermal environment.

#### Acknowledgement

This work was jointly supported by the National Key Research Program of China (No. 2014CB953900), the National Natural Science Foundation of China (No. 41375081), and the Sun Yat-sen University “985 Project” Phase 3. We acknowledge

Prof. Su Z. (Bob) of the Faculty of Geo-Information Science and Earth Observation (ITC), University of Twente and Dr. Claudia Künzer of German Remote Sensing Data Center, German Aerospace Center (DLR) for their valuable advices and assistance during the preparation of this paper. We appreciate the efforts provided by Prof. Wu Jianping and Dr. Hu Kezhen of Tsinghua University during the paper revision. The comments from two anonymous reviewers benefit the paper. We thank all the data providers and our previous collaborators for related investigations.

#### REFERENCES

- Arvidson, T., Barsi, J.A., Jhabvala, M., Reuter, D., 2013. Landsat and thermal infrared imaging. In: Kuenzer, C., Dech, S. (Eds.), *Thermal Infrared Remote Sensing: Sensors, Methods, Applications*. Springer, Netherlands: pp. 177–196. [http://dx.doi.org/10.1007/978-94-007-6639-6\\_9](http://dx.doi.org/10.1007/978-94-007-6639-6_9).
- Baldrige, A.M., Hook, S.J., Grove, C.I., Rivera, G., 2009. The ASTER spectral library version 2.0. *Remote Sens. Environ.* 113:711–715. <http://dx.doi.org/10.1016/j.rse.2008.11.007>.
- Barsi, J.A., Hook, S.J., Palluconi, F.D., Schott, J.R., Raqueno, N.G., 2006. Landsat TM and ETM+ thermal band calibration. *Proceedings of SPIE International Symposium, San Diego, CA, 7 September*.
- Barsi, J.A., Hook, S.J., Schott, J.R., Raqueno, N.G., Markham, B.L., 2007. Landsat-5 thematic mapper thermal band calibration update. *IEEE Geosci. Remote Sens.* 4 (4), 552–555.
- Barsi, J.A., Schott, J.R., Hook, S.J., Raqueno, N.G., Markham, B.L., Radocinski, R.G., 2014. Landsat-8 thermal infrared sensor (TIRS) vicarious radiometric calibration. *Remote Sens.* 6 (11): 11607–11626. <http://dx.doi.org/10.3390/rs6111607>.
- Buyantuyev, A., Wu, J., 2010. Urban heat islands and landscape heterogeneity: linking spatiotemporal variations in surface temperatures to land-cover and socioeconomic patterns. *Lands. Ecol.* 25 (1):17–33. <http://dx.doi.org/10.1007/s10980-009-9402-4>.
- Camacho, F., Cernicharo, J., Lacaze, R., Baret, F., Weiss, M., 2013. GEOV1: LAI, FAPAR essential climate variables and FCOVER global time series capitalizing over existing products. Part 2: validation and intercomparison with reference products. *Remote Sens. Environ.* 137 (10), 310–329.
- Chander, G., Markham, B.L., Helder, D.L., 2009. Summary of current radiometric calibration coefficients for Landsat MSS, TM, ETM+, and EO-1 ALI sensors. *Remote Sens. Environ.* 113, 893–903.
- Chen, F., He, B.Y., Long, Z.Y., Yang, X.Q., 2008. A spatial analysis of urban heat island and underlying surface using Landsat ETM+. *Remote Sens. Land Resour.* (2), 56–61.
- Chen, F., Xiong, Y.Z., Huang, S.P., Ye, H., 2010a. Spatial heterogeneity of atmospheric water vapor and its influence on the retrieval of land surface temperature based on remote sensing data. *Remote Sens. Land Resour.* (2), 35–40.
- Chen, F., Tang, L.N., Qiu, Q.Y., Wang, C.P., 2010b. Exploitation of CBERS-02B as auxiliary data in recovering the Landsat7 ETM+ SLC-off image. *Proceedings of 18th International Conference on GeoInformatics, Beijing, China, 18–20 June* (DOI: 10.1109/GEOINFORMATICS.2010.5567696).
- Chen, F., Zhao, X.F., Ye, H., Hu, H.Y., 2011a. Retrieving land surface temperature from Landsat TM using different atmospheric products as ancillary data. *Proceedings of ICSDM & BJ-IWGIS 2011, Fuzhou, China, 29 June–1 July*.
- Chen, F., Tang, L.N., Wang, C.P., Qiu, Q.Y., 2011b. Recovering of the thermal band of Landsat 7 SLC-off ETM+ image using CBERS as auxiliary data. *Adv. Space Res.* 48 (6):1086–1093. <http://dx.doi.org/10.1016/j.asr.2011.05.012>.

- Chen, J., Zhu, X., Vogelmann, J.E., Gao, F., Jin, S., 2011c. A simple and effective method for filling gaps in Landsat ETM+ SLC-off images. *Remote Sens. Environ.* 115, 1053–1064.
- Chen, F., Zhao, X.F., Ye, H., 2012. Making use of the Landsat 7 SLC-off ETM+ image through different recovering approaches. In: Karakehayov, Zdravko (Ed.), *Data Acquisition Applications*. InTech, Croatia, pp. 317–342.
- Chen, F., Yang, S., Liu, L., Zhao, X.F., 2014a. The new single-channel approaches for retrieving land surface temperature and the preliminary results. In: Xiong, X., Shimoda, H. (Eds.), *Proceedings of SPIE 9264, Earth Observing Missions and Sensors: Development, Implementation, and Characterization III*. SPIE, USA, p. 926414.
- Chen, F., Zhao, X.F., Quan, Y., Liu, L., 2014b. A single-channel method based on temporal and spatial information (MTSC) for retrieving land surface temperature from remote sensing data. *J. Remote Sens.* 18 (3), 657–672.
- Chen, F., Yang, S., Su, Z., He, B.Y., 2015. A new single-channel method for estimating land surface temperature based on the image inherent information: the HJ-1B case. *ISPRS J. Photogramm.* 101, 80–88.
- Chen, F., Yang, S., Su, Z., Wang, K., 2016a. Effect of emissivity uncertainty on surface temperature retrieval over urban areas: investigations based on spectral libraries. *ISPRS J. Photogramm.* 114, 53–65.
- Chen, F., Yin, S.J., Zhu, L., Yin, K., He, B.Y., Yang, S., 2016b. Radiometric calibration of the HJ-1B thermal channel and its effects on land surface temperature retrieval. *J. Remote Sens.* 20 (4), 1993–2002.
- Gluch, R., Quattrochi, D.A., Luvall, J.C., 2006. A multi-scale approach to urban thermal analysis. *Remote Sens. Environ.* 104 (2):123–132. <http://dx.doi.org/10.1016/j.rse.2006.01.025>.
- Hollmann, R., Merchant, C.J., Saunders, R., et al., 2013. The ESA climate change initiative: satellite data records for essential climate variables. *Bull. Am. Meteorol. Soc.* 94 (14):1541–1552. <http://dx.doi.org/10.1016/j.rse.2011.09.022>.
- Hu, H.Y., Chen, F., Wang, Q.C., 2011. Estimating the effective wavelength of the thermal band for accurate brightness temperature retrieval: methods and comparison. *Proceedings of ICSDM & BJ-IWGIS 2011*, Fuzhou, China, 29 June–1 July.
- Jiménez-Muñoz, J.C., Sobrino, J.A., 2003. A generalized single-channel method for retrieving land surface temperature from remote sensing data. *J. Geophys. Res.* 108 (D22):4688. <http://dx.doi.org/10.1029/2003JD003480>.
- Jiménez-Muñoz, J.C., Sobrino, J.A., Mattar, C., Franch, B., 2010. Atmospheric correction of optical imagery from MODIS and reanalysis atmospheric products. *Remote Sens. Environ.* 114 (10):2195–2210. <http://dx.doi.org/10.1016/j.rse.2010.04.022>.
- Lagouarde, J.-P., Moreau, P., Irvine, M., Bonnefond, J.-M., Voogt, J.A., Sollic, F., 2004. Airborne experimental measurements of the angular variations in surface temperature over urban areas: case study of Marseille (France). *Remote Sens. Environ.* 93 (4), 443–462.
- Lagouarde, J.-P., Hénon, A., Kurz, B., Moreau, P., Irvine, M., Voogt, J., Mestayer, P., 2010. Modelling daytime thermal infrared directional anisotropy over Toulouse city centre. *Remote Sens. Environ.* 114 (1):87–105. <http://dx.doi.org/10.1016/j.rse.2009.08.012>.
- Li, H., Zeng, Y.-N., Yun, P.-D., Huang, J.-B., Yang, K., Zou, J., 2007. Study on retrieval urban land surface temperature with multi-source remote sensing data. *J. Remote Sens.* 11 (6), 891–898.
- Li, Z.-L., Tang, B.-H., Wu, H., Ren, H.Z., Yan, G.J., Wan, Z.-M., Trigo, I.F., Sobrino, J.A., 2013. Satellite-derived land surface temperature: current status and perspectives. *Remote Sens. Environ.* 131:14–37. <http://dx.doi.org/10.1016/j.rse.2012.12.008>.
- Li, P., Jiang, L.G., Feng, Z.M., 2014. Cross-comparison of vegetation indices derived from Landsat-7 enhanced thematic mapper plus (ETM+) and Landsat-8 operational land imager (OLI) sensors. *Remote Sens.-Basel* 6:310–329. <http://dx.doi.org/10.3390/rs6010310>.
- Liu, H., Weng, Q.H., 2009. Scaling effect on the relationship between landscape pattern and land surface temperature: a case study of Indianapolis, United States. *Photogramm. Eng. Remote Sens.* 75 (3), 291–304.
- Liu, C.G., Lu, X.F., Gao, S.F., 2011. Comparison of brightness temperatures inverted from high and low gain state data of Landsat-7 ETM+ thermal infrared band. *J. Henan Polytech. Univ. (Nat. Sci.)* 30 (5), 561–566.
- Loomis, J., Koontz, S., Miller, H., Richardson, L., 2015. Valuing geospatial information: using the contingent valuation method to estimate the economic benefits of Landsat satellite imagery. *Photogramm. Eng. Remote Sens.* 81 (8), 647–656.
- Loveland, T.R., Dwyer, J.L., 2012. Landsat: building a strong future. *Remote Sens. Environ.* 122, 22–29.
- Markham, B.L., Helder, D.L., 2012. Forty-year calibrated record of earth-reflected radiance from Landsat: a review. *Remote Sens. Environ.* 122, 30–40.
- Meng, X.H., Lv, S.H., Zhang, T.T., 2007. Testing, improvement and application of MODIS near infrared water vapor products-taking Jinta Oasis in Heihe River Basin as a case study. *J. Infrared Millimeter Waves* 26 (2), 107–111.
- NASA, 2015a. NASA, USGS begin work on Landsat 9 to continue land imaging legacy. Available at: <http://www.nasa.gov/press/2015/april/nasa-usgs-begin-work-on-landsat-9-to-continue-land-imagig-legacy> (Accessed: 15 October 2015).
- NASA, 2015b. Landsat science: Landsat then and now. Available at: <http://landsat.gsfc.nasa.gov/about/> (Accessed: 15 November 2015).
- NASA, 2015c. Land long term data record. Available at: <http://ltdr.nascom.nasa.gov/cgi-bin/ltdr/ltdrPage.cgi> (Accessed: 15 October 2015).
- NOAA, 2015. Climate data record program. Available at: <https://www.ncdc.noaa.gov/cdr> (Accessed: 15 October 2015).
- NRC (National Research Council of the National Academies), 2004. *Climate Data Records from Environmental Satellites: Interim Report*. The National Academies Press, Washington, D.C.
- Oltra-Carrió, R., Sobrino, J.A., Franch, B., Nerry, F., 2012. Land surface emissivity retrieval from airborne sensor over urban areas. *Remote Sens. Environ.* 123, 298–305.
- Pu, R.L., Gong, P., Michishita, R., Sasagawa, T., 2006. Assessment of multi-resolution and multi-sensor data for urban surface temperature retrieval. *Remote Sens. Environ.* 104 (2), 211–225.
- Rizwan, A.M., Dennis, Y.C.L., Liu, C., 2008. A review on the generation, determination and mitigation of Urban Heat Island. *J. Environ. Sci.* 20 (1), 120–128.
- Scaramuzza, P., Micijevic, E., 2004. SLC gap-filled products phase one methodology. Available at [http://landsat.usgs.gov/documents/SLC\\_Gap\\_Fill\\_Methodology.pdf](http://landsat.usgs.gov/documents/SLC_Gap_Fill_Methodology.pdf) (Accessed: 15 October 2015).
- Sobrino, J.A., Oltra-Carrió, R., Sòria, G., Bianchi, R., Paganini, M., 2012. Impact of spatial resolution and satellite overpass time on evaluation of the surface urban heat island effects. *Remote Sens. Environ.* 117:50–56. <http://dx.doi.org/10.1016/j.rse.2011.04.042>.
- Sun, H., Chen, Y.-H., Zhan, W.-F., Wang, M.-J., Ma, W., 2015. A kernel model for urban surface thermal emissivity anisotropy and its uncertainties. *J. Infrared Millimeter Waves* 34 (1), 66–73 (In Chinese).
- Trenberth, K.E., Anthes, R.A., Belward, A., Brown, O., Habermann, T., Karl, T.R., Running, S., Ryan, B., Tanner, M., Wielicki, B., 2013. Challenges of a sustained climate observing system. In: Asrar, G.R., Hurrell, J.W. (Eds.), *Climate Science for Serving Society: Research, Modeling and Prediction Priorities*. Springer, Netherlands, pp. 13–50.
- Trigo, I.F., Peres, L.F., DaCamara, C.C., Freitas, S.C., 2008. Thermal land surface emissivity retrieved from SEVIRI/Meteosat. *IEEE Trans. Geosci. Remote* 46 (2), 307–315.

- USGS, 2013a. Landsat: a global land-imaging mission. Available at: <http://pubs.usgs.gov/fs/2012/3072/> (Accessed: 15 October 2015).
- USGS, 2013b. The final journey of Landsat 5: a decommissioning story. Available at: [http://landsat.usgs.gov/L5\\_Decommission.php](http://landsat.usgs.gov/L5_Decommission.php) (Accessed: 15 October 2015).
- USGS, 2015a. Product guide: Landsat surface reflectance—derived spectral indices version 2.7. Available at: [http://landsat.usgs.gov/documents/si\\_product\\_guide.pdf](http://landsat.usgs.gov/documents/si_product_guide.pdf) (Accessed: 15 October 2015).
- USGS, 2015b. Landsat 8 (L8) data users handbook version 1.0. Available at: <http://landsat.usgs.gov/documents/Landsat8DataUsersHandbook.pdf> (Accessed: 15 October 2015).
- USGS, NASA, 2004. SLC-off gap-filled products gap-fill algorithm methodology: phase 2 gap-fill algorithm. Available at: [www.ga.gov.au/servlet/BigObjFileManager?bigobjid=GA4861](http://www.ga.gov.au/servlet/BigObjFileManager?bigobjid=GA4861) (Accessed: 15 October 2015).
- Valor, E., Caselles, V., 1996. Mapping land surface emissivity from NDVI: application to European, African, and south American areas. *Remote Sens. Environ.* 57 (3), 167–184.
- Voogt, J.A., 2008. Assessment of an urban sensor view model for thermal anisotropy. *Remote Sens. Environ.* 112 (2), 482–495.
- Voogt, J.A., Oke, T.R., 1998. Effects of urban surface geometry on remotely-sensed surface temperature. *Int. J. Remote Sens.* 19 (5), 895–920.
- Voogt, J.A., Oke, T.R., 2003. Thermal remote sensing of urban climates. *Remote Sens. Environ.* 86 (3):370–384. [http://dx.doi.org/10.1016/S0034-4257\(03\)00079-8](http://dx.doi.org/10.1016/S0034-4257(03)00079-8).
- Weng, Q., 2009. Thermal infrared remote sensing for urban climate and environmental studies: methods, applications, and trends. *ISPRS J. Photogramm.* 64 (4), 335–344.
- White-Newsome, J.L., Brines, S.J., Brown, D.G., Dvonch, J.T., Gronlund, C.J., Zhang, K., Oswald, E.M., O'Neill, M.S., 2013. Validating satellite-derived land surface temperature within situ measurements: a public health perspective. *Environ. Health Perspect.* 121 (8), 925–931.
- Woodcock, C.E., Allen, R., Anderson, M., et al., 2008. Free access to Landsat imagery. *Science* 320 (5879):1011. <http://dx.doi.org/10.1126/science.320.5879.1011a>.
- Xiao, R.-B., Ouyang, Z.-Y., Zheng, H., Li, W.-F., Schienke, E.W., Wang, X.-K., 2007. Spatial pattern of impervious surface and their impacts on land surface temperature in Beijing, China. *J. Environ. Sci.* 19 (2):250–256. [http://dx.doi.org/10.1016/S1001-0742\(07\)60041-2](http://dx.doi.org/10.1016/S1001-0742(07)60041-2).
- Xiong, Y.Z., Huang, S.P., Chen, F., Ye, H., Wang, C.P., Zhu, C.B., 2012. The impacts of rapid urbanization on the thermal environment: a remote sensing study of Guangzhou, South China. *Remote Sens.-Basel* 4 (7):2033–2056. <http://dx.doi.org/10.3390/rs4072033>.
- Xu, D.D., Guo, X.L., 2014. Compare NDVI extracted from Landsat 8 imagery with that from Landsat 7 imagery. *Am. J. Remote Sens.* 2 (2), 10–14.
- Yang, J., Wong, M.S., Menenti, M., Nichol, J., 2015. Study of the geometry effect on land surface temperature retrieval in urban environment. *ISPRS J. Photogramm.* 109, 77–87.
- Zeng, Y., Su, Z., Calvet, J.C., et al., 2015. Analysis of current validation practices in Europe for space-based climate data records of essential climate variables. *Int. J. Appl. Earth Obs.* 42: 150–161. <http://dx.doi.org/10.1016/j.jag.2015.06.006>.
- Zha, Y., Gao, J., Ni, S., 2003. Use of normalized difference built-up index in automatically mapping urban areas from TM imagery. *Int. J. Remote Sens.* 24 (3), 583–594.